A Data-centric Approach to Generative Rough Surface Modelling: 3D-printed Stainless Steel

Chris Oates,
Wilfrid Kendall and
Liam Fleming

NEURAL INFORMATION PROCESSING SYSTEMS

3D-printed Stainless Steel Components Exhibit Sizeable Geometric Surface Variations

The 3D printed steel components studied presented a rough banded surface as a result of the manufacturing process. These variations are sufficiently large to impact the macroscale properties of any thin walled components printed. Effective mechanical simulation of these printed structures demands proper surface simulation.

Our Dataset Comprised of 6 High-resolution Laser Scans of Existing Flat Components

The laser scans were subject to a pre-processing procedure to remove global trend data, produced as part of the cutting process, as well as superficial weld splatters which were deemed to have no impact on structural behaviour. The resultant 3D representation was then discretised into matrices which comprised the model training data.

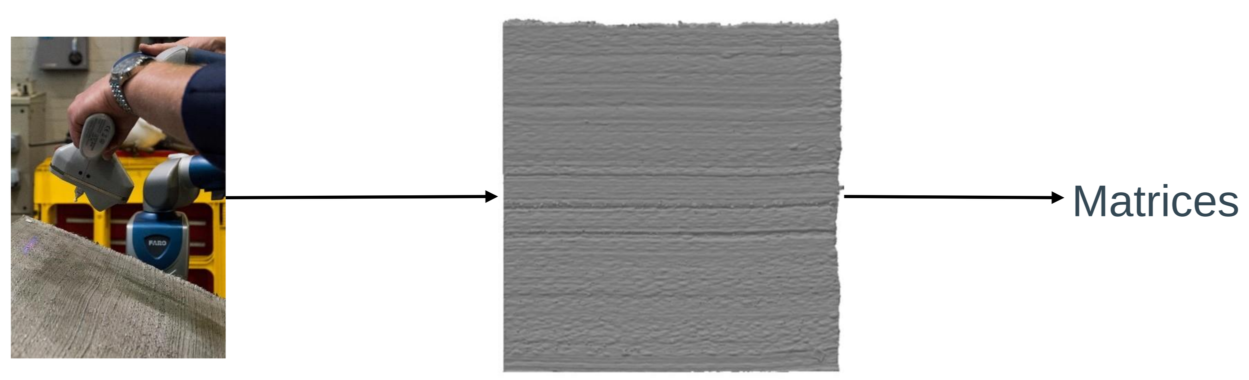

Geometry was Represented by a Pair of Functions Defined on a Manifold to be Modelled by a Bivariate Gaussian Field

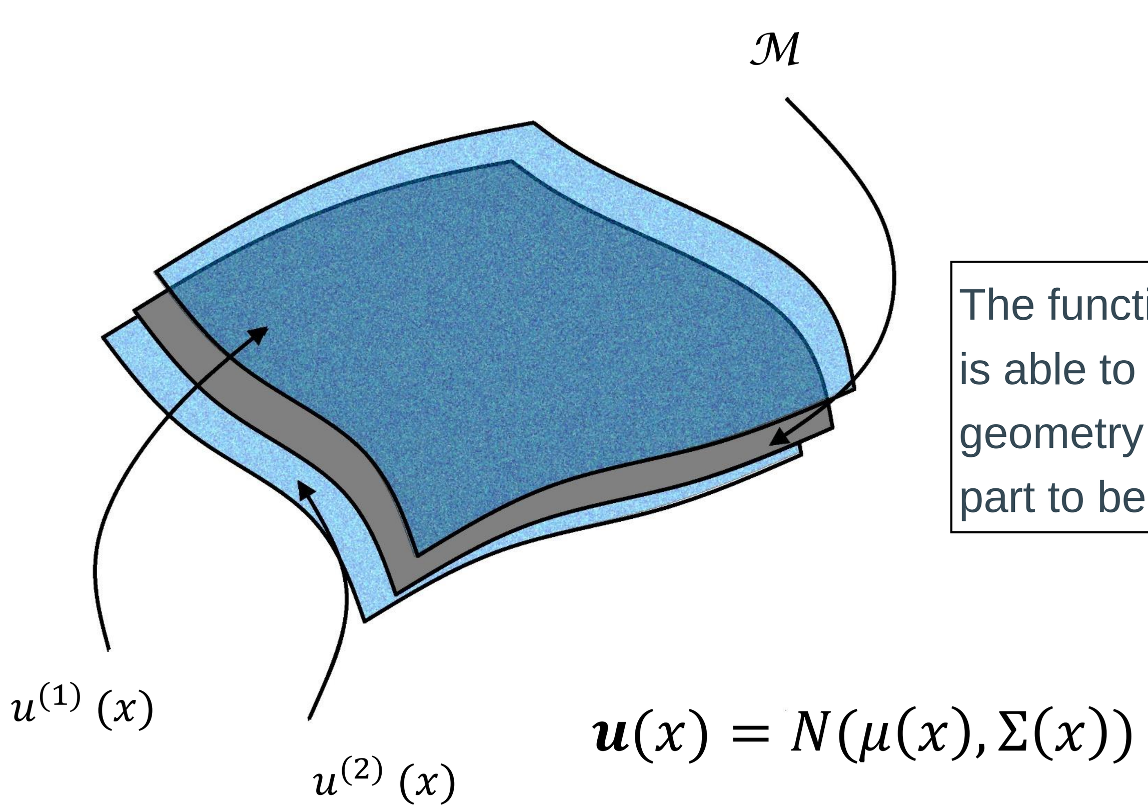

The function pair $(u^{(1)}, u^{(2)})$ is able to fully describe geometry of any theoretical part to be manufactured

$$\boldsymbol{u}(x) = N(\mu(x), \Sigma(x))$$

A Manifold-Agnostic Representation of the Random Field was Required to Simulate to-be-manufactured Parts

This precluded use of the covariance function framework which is inherently manifold-dependent. Instead a representation based on a system of stochastic partial differential equations (SPDEs) was used. A wide range of random fields can be represented by SPDEs with a Laplacian-based differential operator.

$$\begin{bmatrix} \mathcal{L}^{(11)} & \mathcal{L}^{(12)} \\ \mathcal{L}^{(21)} & \mathcal{L}^{(22)} \end{bmatrix} \begin{bmatrix} u^{(1)}(x) \\ u^{(2)}(x) \end{bmatrix} = \begin{bmatrix} Z^{(1)}(x) \\ Z^{(2)}(x) \end{bmatrix}$$

SPDE representation of bivariate Gaussian field for generative model. $\mathcal{L}$ represents differential operators to be specified and Z driving noises derived from a noise process.

Only the Laplacian, $\Delta_{\mathcal{M}}$,is defined locally on the manifold. By associating the Laplacian on one manifold with that on another we are able to use conclusions drawn from one manifold to form the basis of a generative model on the other.

The Choice of Differential Operator and Driving Noise Process is Key to Capturing Features of the Printed Surface.

A selection of candidate differential operators and noise processes were tested and assessed in an Occam's razor fashion using the Akaike Information Criteria (AIC).

Model for $\mathcal{L}^{(rs)}$	**Mathematical Form**
Isotropic Stationary	$\mathcal{L}^{(rs)}u(x) := (\eta^{(rs)} - \Delta)(\tau^{(rs)}u(x))$
Anistropic Stationary	$\mathcal{L}^{(rs)}u(x) := (\eta^{(rs)} - \nabla \cdot \mathbf{H}^{(rs)}\nabla)(\tau^{(rs)}u(x))$
Isotropic Non-stationary	$\mathcal{L}^{(rs)}u(x) := (\eta^{(rs)}(x_3) - \Delta)(\tau^{(rs)}(x_3)u(x))$
Anisotropic Non-stationary	$\mathcal{L}^{(rs)}u(x) := (\eta^{(rs)}(x_3) - \nabla \cdot \mathbf{H}^{(rs)}\nabla)(\tau^{(rs)}(x_3)u(x))$

Candidate Operator forms for $\mathcal{L}^{(rs)}: r, s \in \{1,2\}$. η, τ represent variables to be learned and $\mathbf{H}$ represents a matrix which enables anisotropy in vertical coordinate x_3.

Iso.	**Stat.**	**Noise**	**AIC$\times 10^6$**
✓	✓	white	-2.08
✓	✓	smoother	-2.31
✓	✓	smoother +oscil.	-2.42
✓	✗	white	-1.55
✓	✗	smoother	-2.05
✓	✗	smoother +oscil.	-2.09
✗	✓	white	-2.20
✗	✓	smoother	-2.33
✗	✓	smoother +oscil.	-2.47
✗	✗	white	-1.83
✗	✗	smoother	-2.11
✗	✗	smoother +oscil.	-2.22

The best fit model to the available data was found to be Anisotropic Stationary; driven by a combined smoother and oscillatory noise

A Test Case Matching the Notional Geometry of an Unseen Component Showed "ballpark" Comparability

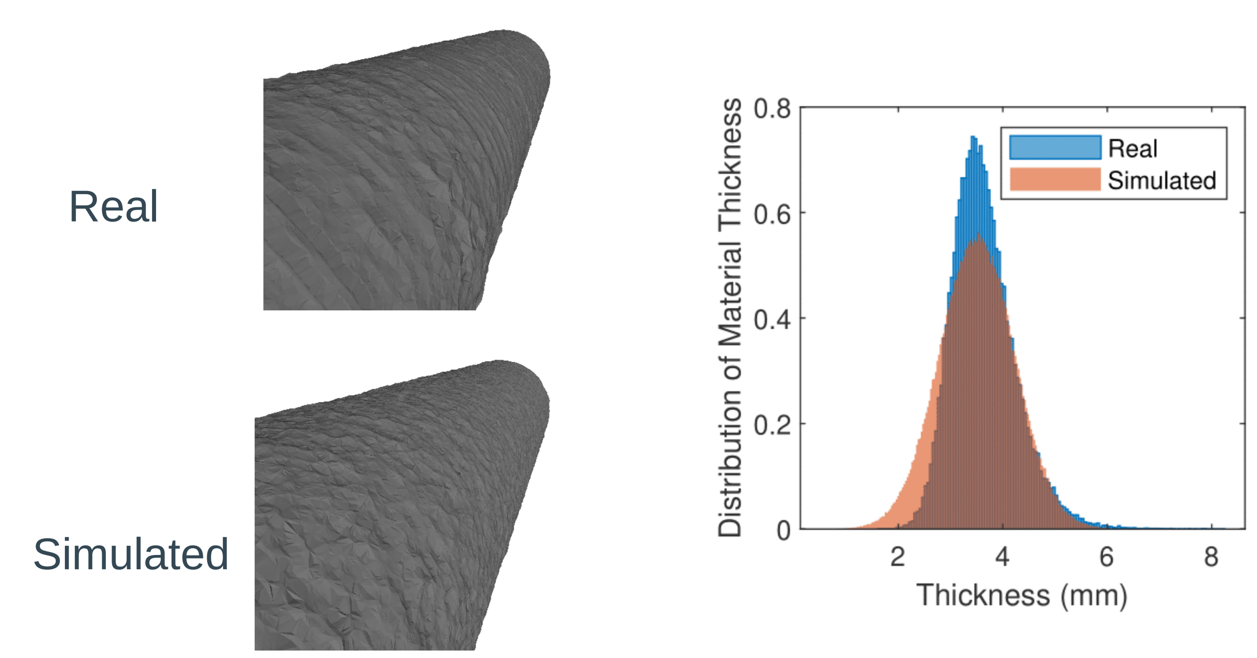

Similarity in the rough surfaces was observed, but our best-fit generative model failed to capture banding and the positive skew in the thickness distribution. Improvement may be obtained with improved characterisation and non-linear transformation of the Gaussian field.

Structural Similarity of the Simulated Columns was Assessed with Buckling Simulation

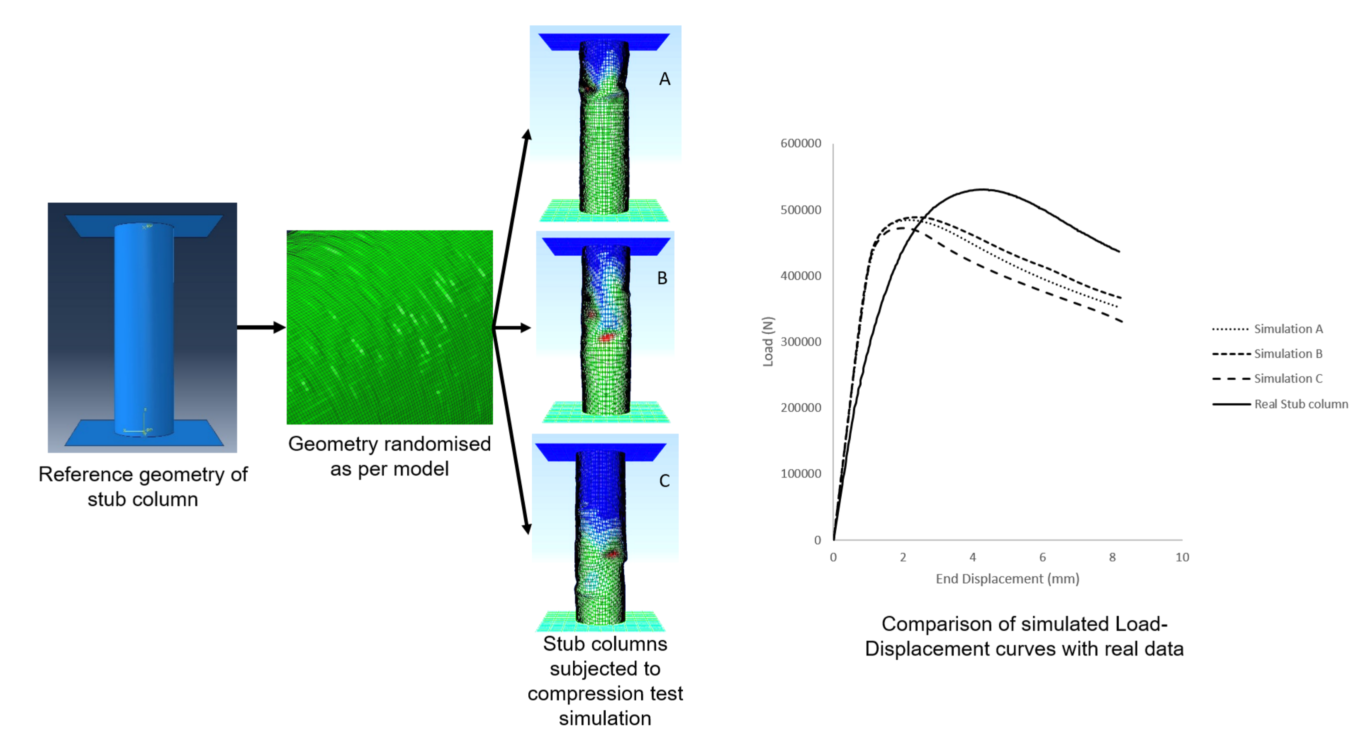

Comparison of simulated Load-Displacement curves with real data

References

C Buchanan and L Gardner. Metal 3d printing in construction: A review of methods, research, applications, opportunities and challenges. Engineering Structures, 180:332–348, 2019.

Tilmann Gneiting. Strictly and non-strictly positive definite functions on spheres. Bernoulli, 19(4):1327–1349, sep 2013.

Xiangping Hu, Finn Lindgren, Daniel Simpson, and Ha°vard Rue. Multivariate Gaussian random fields with oscillating covariance functions using systems of stochastic partial differential equations. arXiv preprint arXiv:1307.1384, 2013.

Finn Lindgren, Ha°vard Rue, and Johan Lindstro¨m. An explicit link between Gaussian fields and Gaussian Markov random fields: the stochastic partial differential equation approach. Journal of the Royal Statistical Society: Series B (Statistical Methodology), 73(4):423–498, 2011.

C.E. Rasmussen and C.K.I. Williams. Gaussian Processes for Machine Learning. MIT Press, 2006.

Sam Davanloo Tajbakhsh, Necdet Serhat Aybat, and Enrique Del Castillo. Sparse precision matrix selection for fitting gaussian random field models to large data sets. arXiv preprint arXiv:1405.5576, 2014.

Tom R Thomas. Rough surfaces. Rough Surfaces, 2nd Edition. Edited by THOMAS TOM R. Published by World Scientific Publishing Co. Pte. Ltd.,. ISBN# 9781860943805, 1999.